Engineering Interfacial Water Activation via Synergistic Defect and Aggregate Carbon Dots Layer for Efficient Nitrate-to-Ammonia Electrocatalysis

*Zhiquan Lang,[#a] Yaxi Li,[#a] Xiangbo Shen,[#b] Naiyun Liu,[*a] Yongchao Du,[a] Yuanyuan Cheng,[a] Chenhe Guo,[a] Xingpeng Liao,[c] Yixing Zhu,[d] Yajun Deng,[e] Jingwen Yu,[a] Yunliang Liu,[a] Longfei Guo,[*f] Zhenhui Kang,[*g] and Haitao Li[*a]*

a. Institute for Energy Research, Jiangsu University, Zhenjiang 212013, China.

b. Shandong Key Laboratory of Intelligent Manufacturing Technology for Advanced Power Equipment, School of Machinery and Automation, Weifang University, Weifang 261061, China.

c. National Engineering Research Center of Light Alloy Net Forming and State Key Laboratory of Metal Matrix Composite, Shanghai Jiao Tong University, Shanghai 200240, China.

d. School of Mechanical Engineering, University of Science and Technology Beijing, Beijing 100083, China.

e. School of Marine Engineering, Jimei University, Xiamen 361021, China

f. Northwest Institute for Non-ferrous Metal Research, Xi'an 710016, China.

g. Institute of Functional Nano and Soft Materials (FUNSOM), Jiangsu Key laboratory for Carbon-based Functional Materials and Devices, Soochow University, Suzhou 215123, China

# These authors contributed equally to this work.

EXPERIMENTAL SECTION

1. Materials. Tantalum pentachloride ($TaCl_5$, ≥99.9%), nitric acid (HNO_3, 14.4 mol L^{-1}), sodium hydroxide (NaOH), potassium nitrate (KNO_3), ethanol (C_2H_5OH), Nafion solution (5 wt%), and DMSO-d6 were purchased from commercial suppliers and used without further purification. Ultrapure water with a resistivity of 18.2 MΩ was used throughout all experiments.

2. Preparation of CDs. To obtain the carbon precursor for constructing the carbon layer in TaON@CL, biomass-derived CDs were synthesized from corn straw, and part of their structural features were later preserved within the carbon layer of the final composite. CDs were synthesized from corn straw powder using a hydrothermal method. First, 5 g of dried and pulverized straw was refluxed in 200 mL of 14.4 mol L^{-1} HNO_3 under N_2 atmosphere at 60 °C for 12 h. The mixture was filtered through a 0.45 μm membrane, washed thoroughly with deionized water, and dried in a vacuum oven at 60 °C for 12 h. Then, 200 mg of the nitrated product was dispersed in 50 mL of 1 mol L^{-1} NaOH and subjected to hydrothermal treatment at 160 °C for 20 h. The product was purified using a 3,500 Da dialysis membrane for 12 h and freeze-dried to yield yellow CDs powder.

3. Preparation of Ta_2O_5. Ta_2O_5 was prepared by spray-drying a $TaCl_5$ ethanol solution followed by thermal treatment. Specifically, 358.41 mg of $TaCl_5$ was dissolved in 150 mL of anhydrous ethanol and stirred for 30 min, followed by the rapid addition of 350 mL of deionized water. The resulting mixture was spray-dried (inlet temperature: 150 °C, feed rate: 15%, air flow: 50%, atomization rate: 600 mL min^{-1}) to obtain a white precursor powder, which was then calcined in Ar at 900 °C for 5 h to yield crystalline Ta_2O_5.

4. Preparation of TaON. TaON was synthesized from the same Ta precursor via ammonolysis.

The spray-dried $TaCl_5$-derived powder (as in Section 2.3) was annealed in flowing NH_3 at 900 °C for 10 h, inducing nitridation and generating oxygen vacancies. The resulting TaON powder was collected and stored in a desiccator before further use.

5. Preparation of TaON@CL. To prepare the TaON@CL hybrid, 50 mg of TaON powder was mixed with 30 mL of 1 mg mL^{-1} CDs aqueous solution. The mixture was subjected to microwave irradiation at 300 W for 20 min. After reaction, the product was washed with deionized water and ethanol, followed by drying at 60 °C to yield the TaON@CL composite catalyst.

6. Electrocatalytic experiment. Electrochemical nitrate reduction tests were carried out in a standard H-type two-chamber cell using a CHI660E electrochemical workstation. The working electrode was prepared by dispersing 2.5 mg of catalyst in 480 μL of 75% ethanol containing 20 μL of 5% Nafion solution. After sonication for 30 min, 50 μL of the suspension was drop-cast onto 1 cm^2 of carbon paper and dried under ambient conditions. A platinum foil and a saturated calomel electrode (SCE) served as the counter and reference electrodes, respectively. The electrolyte in the cathode chamber consisted of 35 mL of 1 M KOH with 0.1 M KNO_3. A FAB-PK-130 anion exchange membrane separated the cathode and anode compartments. Prior to measurements, the electrodes were activated via cyclic voltammetry (CV) scanning until a stable curve was achieved. All potentials were converted to the reversible hydrogen electrode (RHE) scale using the equation:

$$E\ (\text{vs. RHE}) = E\ (\text{vs. SCE}) + 0.242 + 0.059 \times \text{pH}$$

Chronoamperometry was performed at various potentials for 1 h with continuous stirring at 300 rpm. Post-electrolysis, the electrolyte was analyzed for NH_3 and NO_2^- concentrations using Nessler's reagent and Griess reagent, respectively. The ammonia yield and Faradaic efficiency were calculated

based on UV–vis absorbance.

7. DFT calculations. All spin-polarized DFT calculations were conducted using the Vienna ab initio simulation (VASP) package with the projector-augmented wave (PAW) approach.[1, 2] The exchange–correlation interactions were described using the Perdew–Burke–Ernzerhof (PBE) functional of the generalized gradient approximation (GGA).[3] Electronic occupancies were treated using the Gaussian smearing method with a width of 0.05 eV. The van der Waals interactions were incorporated via the DFT-D3 correction.[4] The plane-wave energy cutoff of 450 eV was employed for the expansion of the electronic wave functions. The energy convergence criterion was set to less than 10–5 eV, and the residual force on each atom during ionic relaxation was less than 0.05 eV/Å. Brillouin zone integrations were carried out using a 2 × 2 × 1 Monkhorst–Pack *k*-point mesh. To avoid artificial interactions between periodic images, a vacuum layer of 15 Å was introduced along the z-direction.

The Gibbs free energy change of each elementary reaction step during NitRR was evaluated according to the equation:

$$G = E_{elec} + E_{ZPE} - TS$$

where the E_{elec} represents the DFT-calculated electronic energy at 0 K, E_{ZPE} denotes the zero-point energy correction, and the temperature T was set to 298.15 K.

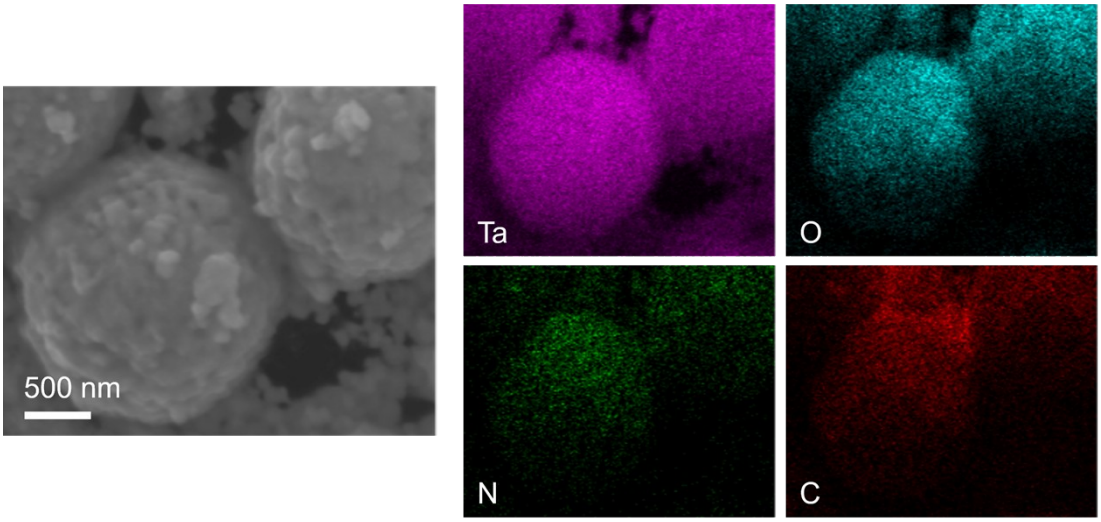

Fig. S1. EDS mapping of TaON@CL.

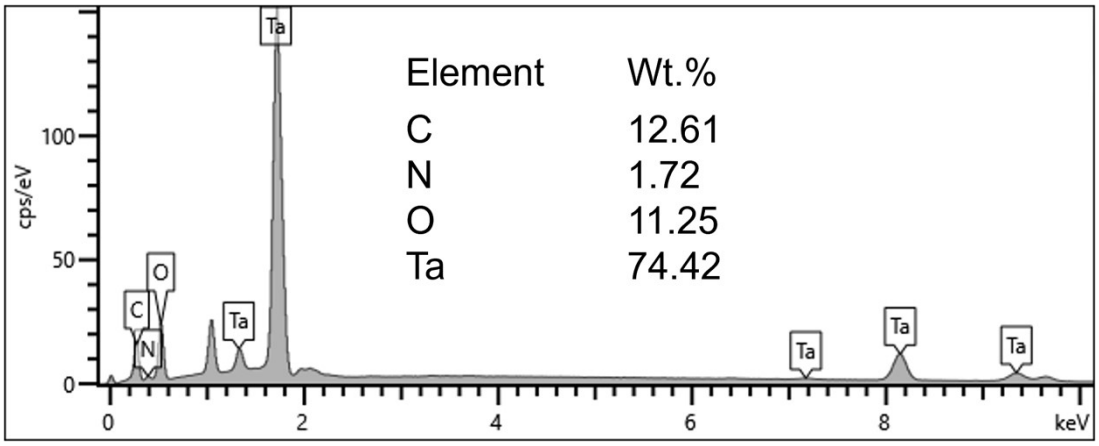

Fig. S2. EDS result of TaON@CL.

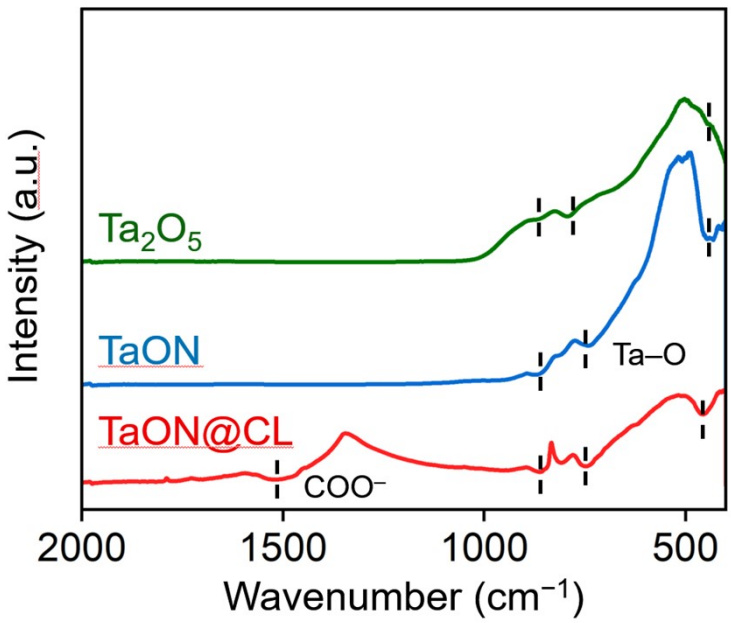

Fig. S3. FT-IR spectra of Ta_2O_5, TaON, and TaON@CL.

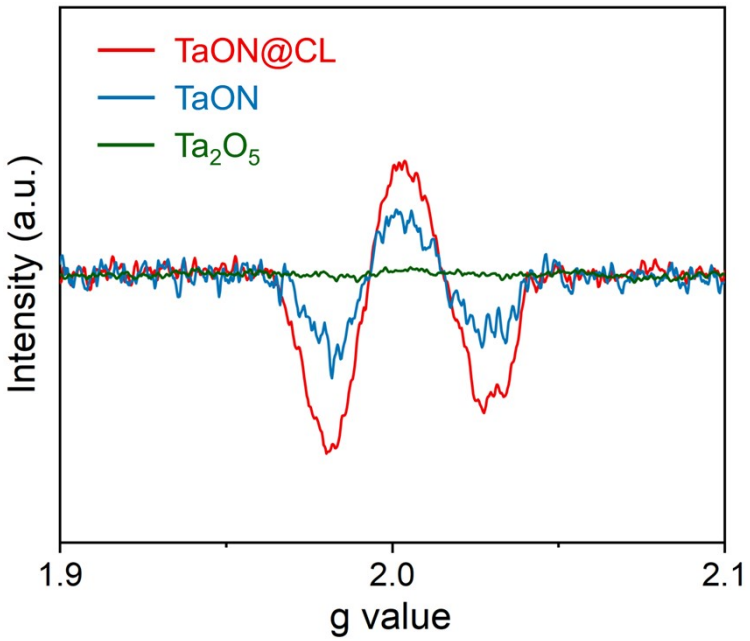

Fig. S4. EPR spectra of Ta_2O_5, TaON, and TaON@CL.

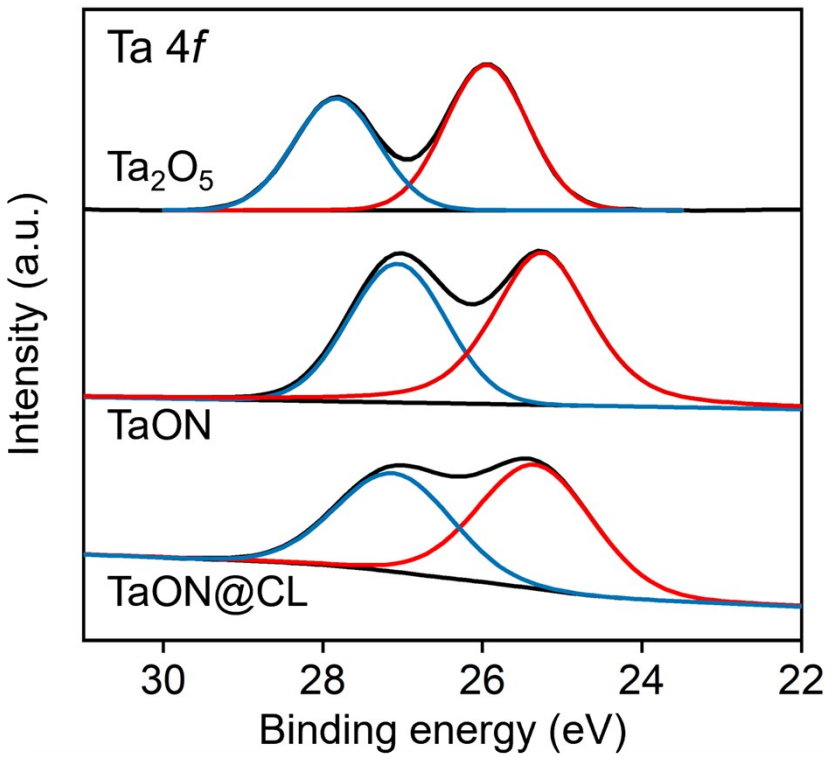

Fig. S5. Ta 4*f* XPS spectra of Ta_2O_5, TaON, and TaON@CL.

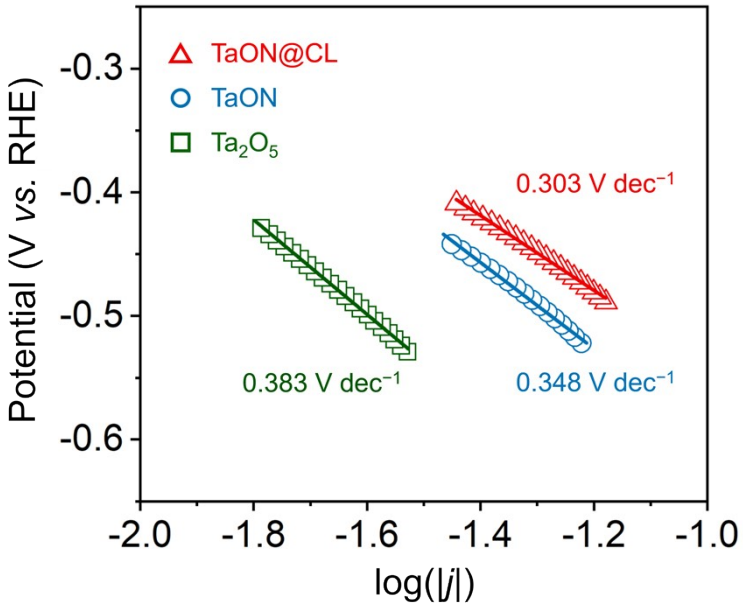

Fig. S6. Tafel plots of Ta_2O_5, TaON, and TaON@CL catalysts.

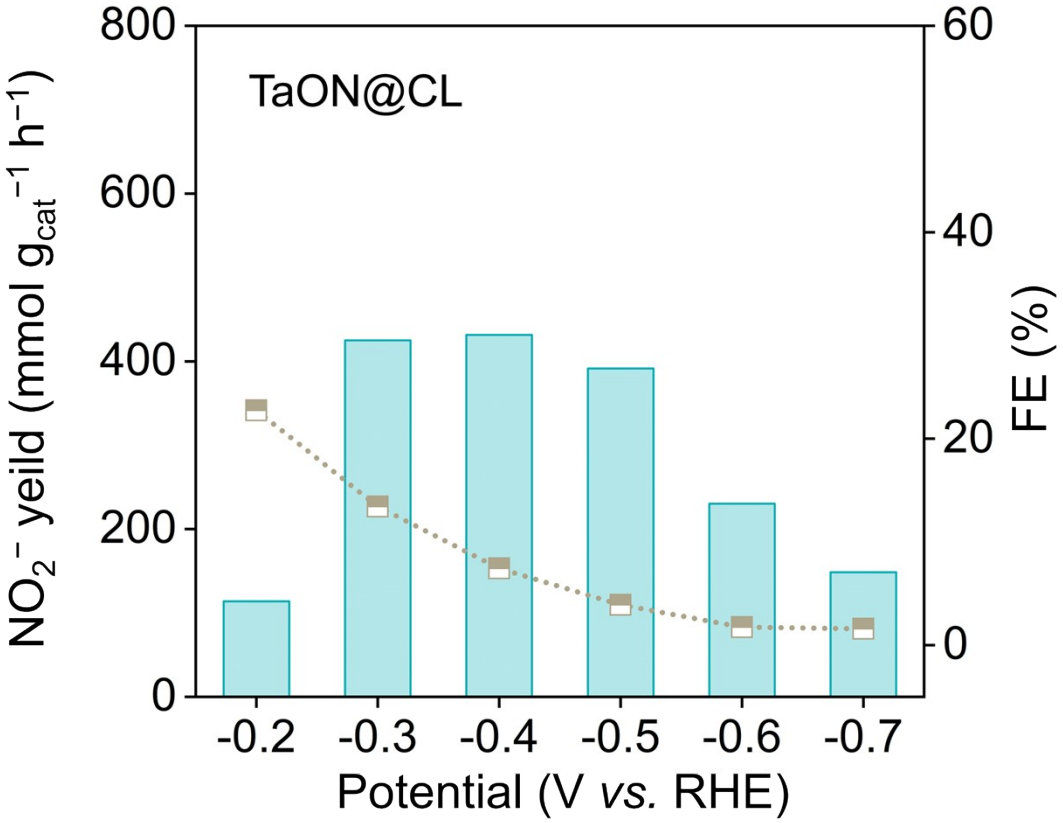

Fig. S7. Yield and Faraday efficiency of NO_2^- of TaON@CL at different potentials.

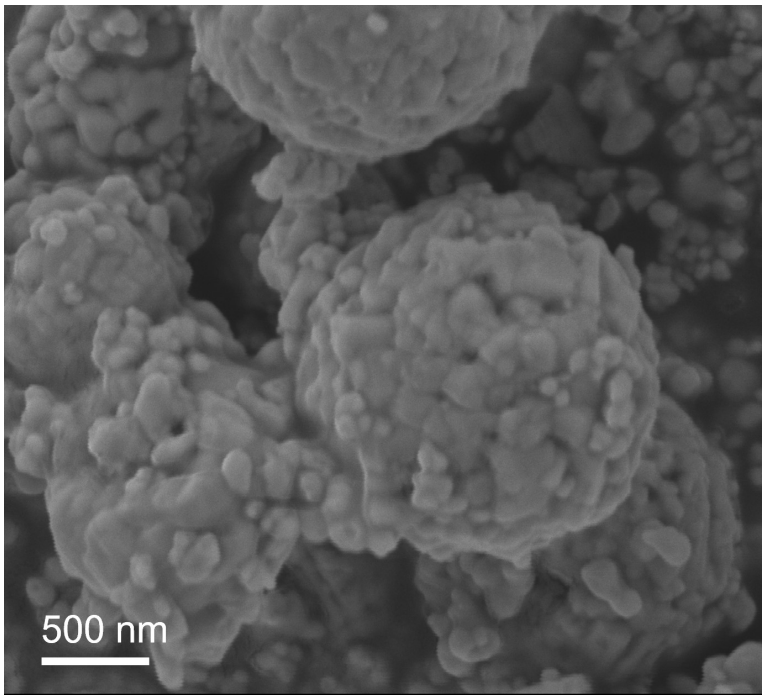

Fig. S8. SEM image of TaON@CL after stability test.

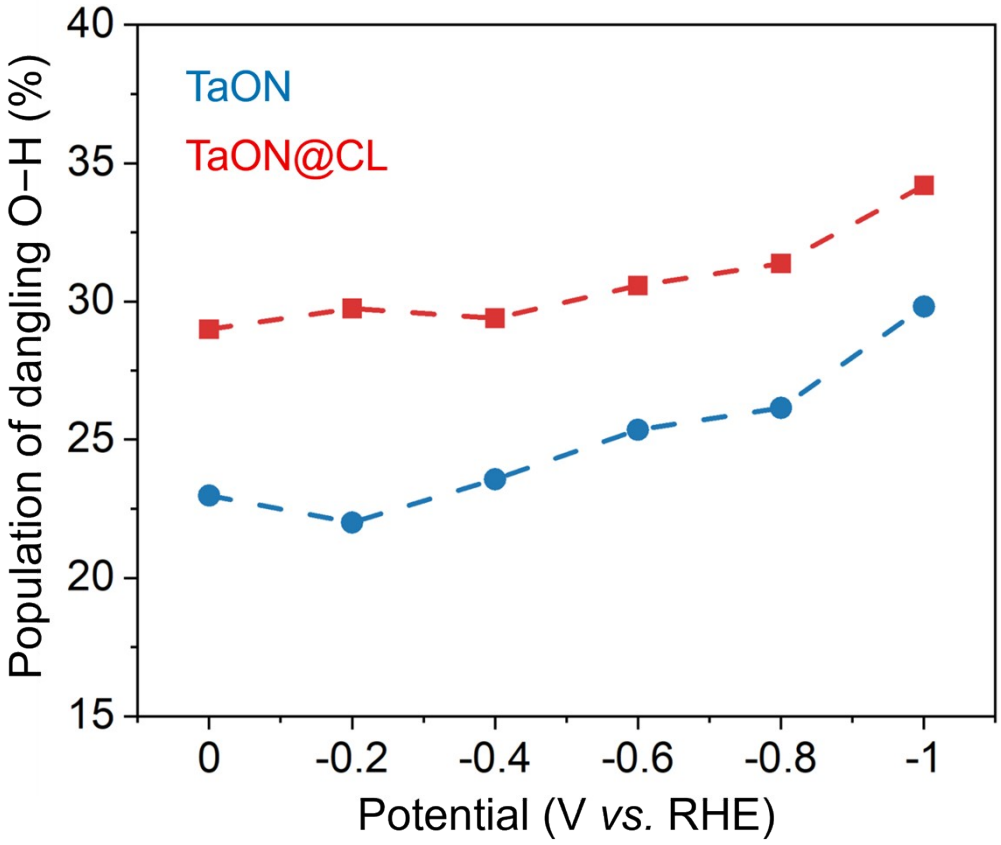

Fig. S9. Proportion of dangling O−H of TaON@CL and TaON at different potentials.

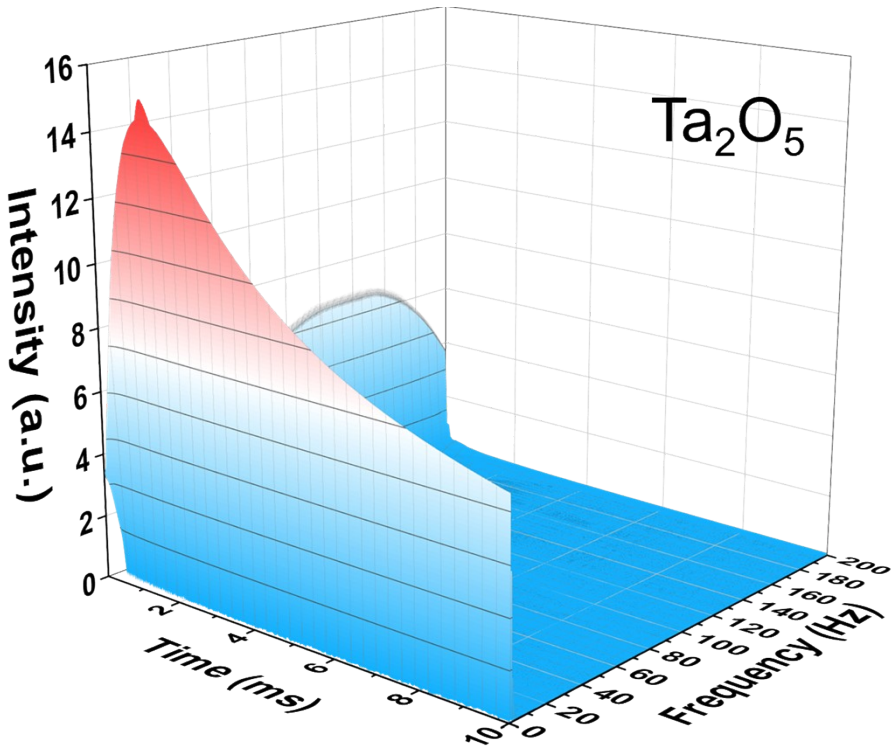

Fig. S10. 3D CWT patterns of Ta_2O_5.

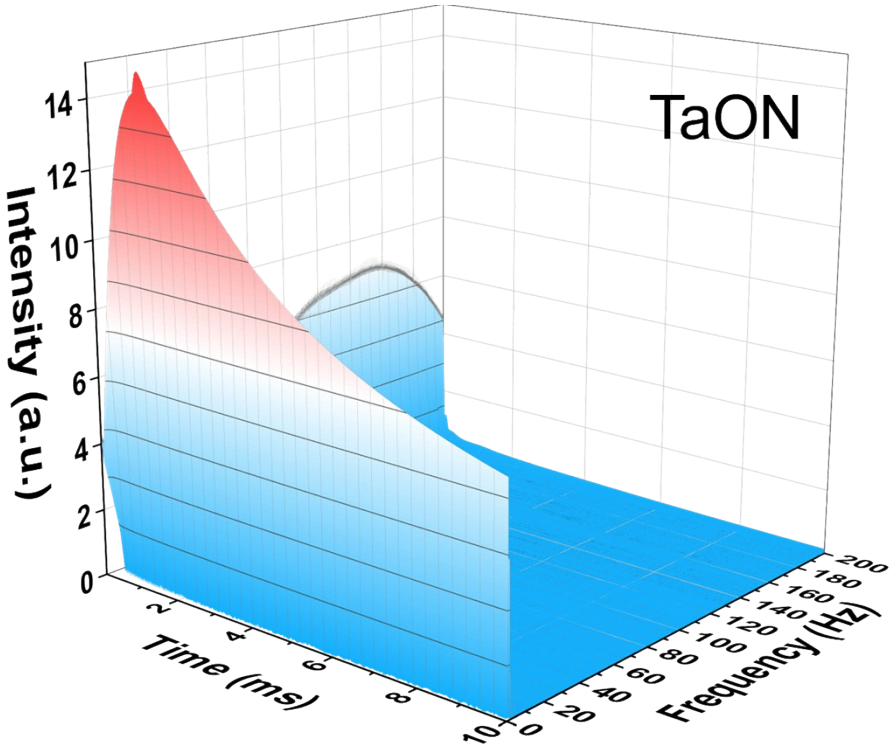

Fig. S11 3D CWT patterns of TaON.

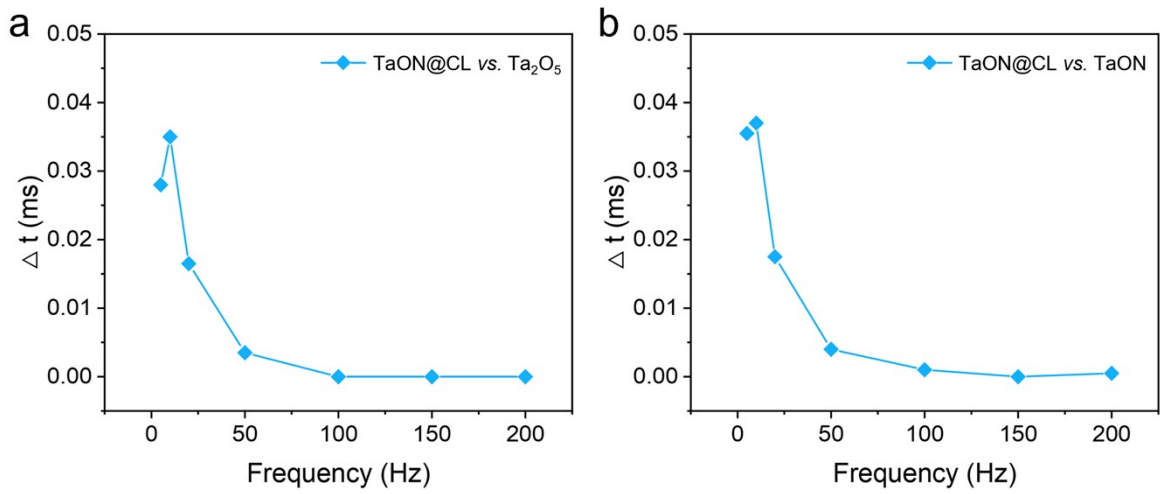

Fig. S12. Comparison of the peak occurrence time of TaON@CL with those of (a) TaON and (b) Ta_2O_5 at different frequencies (10Hz, 20 Hz, 50 Hz, 100 Hz, 150 Hz, and 200 Hz).

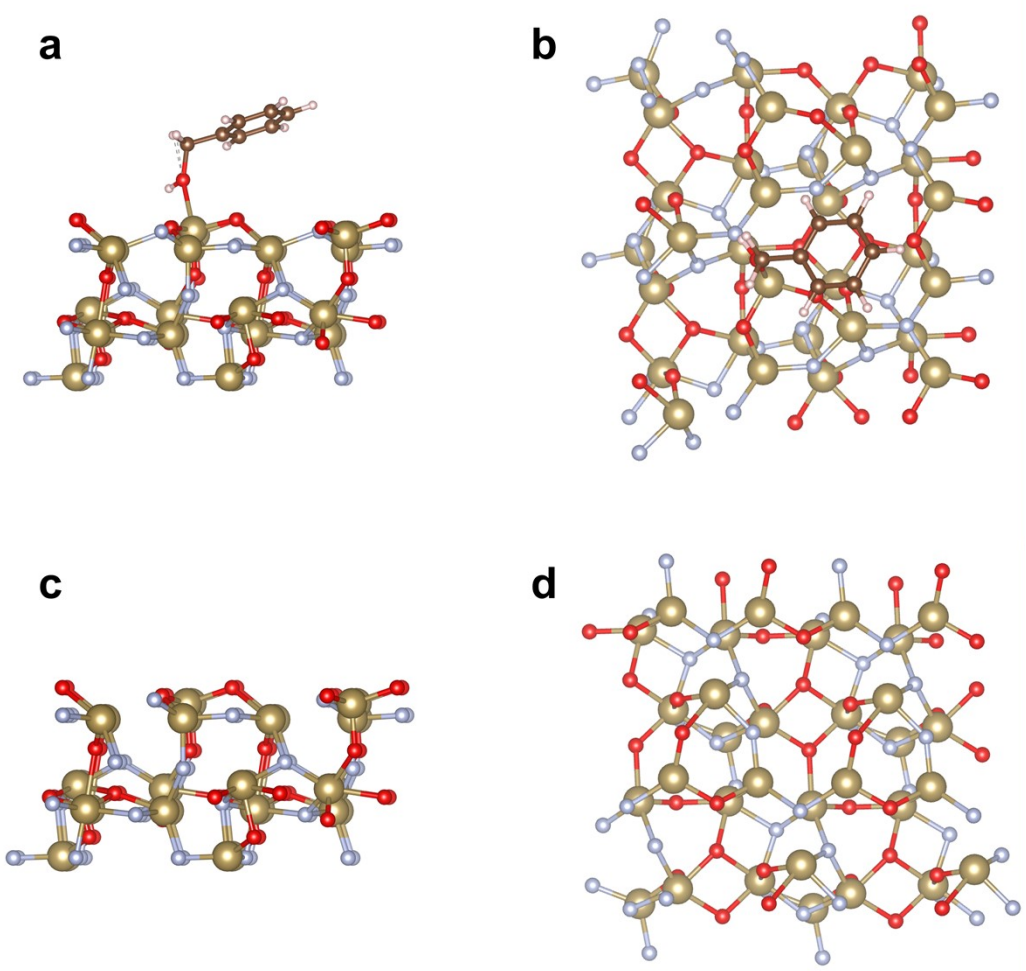

Fig. S13. Side and top view of TaON@CL (a, b) and TaON (c, d).

Table 1: Synchronous–asynchronous correlation matrix of TaON@CL showing peak evolution order.

	NO_3	NO_2	NH_2OH	NH_3
NO_3	/	(−,−)	(+,+)	(+,+)
NO_2		/	(−,−)	(−,−)
NH_2OH			/	(+,−)
NH_3				/

NO_3: 1370 cm^{-1}

NO_2: 1205 cm^{-1}

NH_2OH: 1103 cm^{-1}

NH_3: 1478 cm^{-1}

Reference

1. G. Kresse and J. Furthmüller, Efficiency of ab-initio total energy calculations for metals and semiconductors using a plane-wave basis set, *Comput. Mater. Sci.*, 1996, **6**, 15-50.

2. G. Kresse and J. Furthmüller, Efficient iterative schemes for ab initio total-energy calculations using a plane-wave basis set, *Phys. Rev. B*, 1996, **54**, 11169.

3. J. P. Perdew, K. Burke and M. Ernzerhof, Generalized Gradient Approximation Made Simple, *Phys. Rev. Lett.*, 1996, **77**, 3865.

4. S. Grimme, Semiempirical GGA-type density functional constructed with a long-range dispersion correction, *J. Comput. Chem.*, 2006, **27**, 1787-1799.